

# EFFECTS OF REYNOLDS NUMBER AND ADVERSE PRESSURE GRADIENT ON A TURBULENT BOUNDARY LAYER DEVELOPING ON A ROUGH SURFACE

Guy Pailhas

Yann Touvet

Bertrand Aupoix

Department of Modelling for Aerodynamics and Energetics,  
ONERA  
2, Av Edouard Belin BP7 4025 31055 Toulouse, France  
[guy.pailhas@onera.fr](mailto:guy.pailhas@onera.fr)

## ABSTRACT

A detailed experimental study of turbulent boundary layers developing over rough surfaces and submitted to both zero and adverse pressure gradient was undertaken. Two surface roughness characterized by distributed random elements have been chosen. The boundary layer was probed with a single hot wire in order to get mean and turbulent quantities. Skin friction coefficient was obtained from the semi-logarithmic profiles of the mean velocity, using laws of the wall.

The emphasis of this work is on the dependency of the “equivalent sand roughness” upon the pressure gradient and the Reynolds number. It was pointed out that both the roughness topology and the nature of flow had to be taken into account when the equivalent sand roughness concept was needed.

## INTRODUCTION

The knowledge of friction and heat transfer characteristics between the flow and the solid surface remains essential in a great number of applications. The dynamics of the flow and its thermal characteristics are directly affected by the geometry of the immersed solid but also by its surface roughness. Even if most of basic turbulent research concerns the structure of the flow over a smooth surface, rough surface effects have received an increased attention in the past several years. There are a host of industrial motivations for research on rough-wall boundary layers.

Up to now, two distinct approaches are used to represent the effects of wall distributed roughness on a developing turbulent boundary layer: the classical equivalent-sand-grain roughness approach proposed by Schlichting from Nikuradse works and the discrete element approach. The main drawback of the former approach is that the equivalent-sand-grain roughness for a specific surface is determined from empiric correlations (as Dirling’s or Grabow and White’s) based on geometric considerations only. In the latter approach, roughness must be represented by distributed sources and sinks in the various governing

equations that needs to modify deeply the Navier-Stokes equations. Only the equivalent-sand-grain roughness concept can be used in industrial, general purpose, Navier-Stokes solvers.

The computation of experiments performed at MSU, over regularly distributed hemispheres, showed that the required equivalent-sand-grain roughness may depend not only on the geometry but also on the flow regime (Aupoix and Spalart, 2003). So, an experimental study was conducted varying the wall roughness, the Reynolds number and the pressure gradient.

## EQUIVALENT SAND ROUGHNESS

The first experiments on rough surfaces were conducted in pipes or rectangular ducts by Darcy (1858) and Bazin (1902). They observed the roughness effect on the velocity profile and laid down correlations between the friction factor, the Reynolds number and the roughness height. Nikuradse (1933) completed predecessor works investigating flow in sand-roughened pipes. He proposed the following form for the logarithmic law:

$$\frac{u}{u_\tau} = \frac{1}{\kappa} \ln\left(\frac{y}{h}\right) + B(h^+)$$

with  $h^+ = \frac{hu_\tau}{\nu}$ , the roughness Reynolds number based upon the roughness height  $h$ .

This logarithmic law of the mean velocity profile across the turbulent boundary layer is usually written as:

$$\frac{u}{u_\tau} = \frac{1}{\kappa} \ln\left(\frac{yu_\tau}{\nu}\right) + C - \Delta u^+(h^+)$$

where  $\Delta u^+ = \frac{\Delta u}{u_\tau}$  represents the downward shift of the semi-logarithmic region with reference to a smooth surface.

Nikuradse identified three regimes for fully developed rough flows, using  $h^+$  as flow regime delimiter:

- hydrodynamically smooth  $h^+ < 4$
- transitionally rough  $4 < h^+ < 70$
- fully rough  $h^+ > 70$

Later, Schlichting (1937) studied the effects on the flow of roughness elements varying their size, shape and density. The roughness elements consisted of hemispheres, spherical segments, cones wedges and sand grains. He introduced the concept of a single length scale descriptor of surface roughness; he defined  $h_s$  as the equivalent sand grain roughness height in Nikuradse experiment which provides the same skin friction increase that a particular rough surface. The data of Schlichting's experiments conducted on surface with hemispheres, conical segments or cones as rough elements indicate that the spacing parameter  $l/h$  with  $l$  defined as the inverse square root of the number of roughness element per unit surface could be correlated with the ratio  $h_s/h$ . The main problem is how to determine  $h_s$  when no skin friction data are available for a specific rough surface.

From various experimental results, Dirling (1973) showed that the inclination of the roughness element, connected to the three-dimensionality of the roughness element shape, was also an important correlating parameter. He proposed to correlate  $h_s/h$  in term of :

$$\Lambda = \frac{l}{h} \left( \frac{A_s}{A_p} \right)^{4/3}$$

where  $A_s$  is the windward surface area of the rough element and  $A_p$  the projected area in the direction of the flow. This correlation allowed  $h_s$  to be determined from geometric characteristics of the roughness strictly.

Though a large degree of uncertainty exists in the valuation of  $h_s$ , most calculation procedures rely on the knowledge of the equivalent sand grain roughness.

## EXPERIMENTAL SET-UP AND INVESTIGATED CASES

The experiments were conducted in DMAE subsonic wind tunnel. This research facility is a continuous wind tunnel with a rectangular test section size 0.40 m wide by 0.30 m high and 1.20 m long. The wind tunnel is designed to perform tests varying the velocity from 0 to 70  $\text{ms}^{-1}$ .

Three flow patterns were created: a zero and two moderate and strong adverse pressure gradient flows. The zero pressure gradient conditions (ZPG) were obtained in the boundary layer flow developing on a plate located horizontally 50 mm above the test section floor. To generate an adverse pressure gradient (APG), a flat plate fitted with a movable flap device (FD) was located at half of the test section height. To get a more decelerated flow and come near to separation, this experimental setup (figure 1) was then removed and replaced by a bump device (BD) located 111 mm above the test section wall.

Boundary layer probing were performed on the horizontal plate at eleven X-stations (X01 to X11) from X=0 mm taken at 690 mm downstream the leading edge of the plate (corresponding to the beginning of the flow slowing-down phase in APG configuration) to X=300 mm by 30 mm step. The surface of the plate was wholly smooth or rough. Two rough surfaces (*rug1* and *rug2*) were tested. In general case (C1), measurements were performed at a

reference velocity of 30  $\text{ms}^{-1}$  corresponding to a Reynolds number (based on a 1m reference length) of  $2 \cdot 10^6$ . The range of the Reynolds number based on the momentum thickness was 2200-5800 and 3200-3800 respectively with and without pressure gradient in smooth configuration.

The flow developing in ZPG on the rough surface *rug1* was also investigated for a Reynolds number value of  $1 \cdot 10^6$  obtained varying the reference velocity from 30 to 15  $\text{ms}^{-1}$ . This additional case was named C2. A summary of the experimental conditions is presented in table 2.

The main mean velocity and turbulence traverses were carried out in the centre plane of the tunnel using single hot wire probe.

| Pressure Gradient | Experimental device | Reference surface | Test case        |
|-------------------|---------------------|-------------------|------------------|
| ZPG               |                     | smooth            | C1<br>(Re=2 106) |
| ZPG               |                     | <i>rug1</i>       | C1               |
| ZPG               |                     | <i>rug1</i>       | C2<br>(Re=1 106) |
| ZPG               |                     | <i>rug2</i>       | C1               |
| APG               | FD                  | smooth            | C1               |
| APG               | FD                  | <i>rug1</i>       | C1               |
| APG               | BD                  | smooth            | C1               |
| APG               | BD                  | <i>rug1</i>       | C1               |
| APG               | BD                  | <i>rug2</i>       | C1               |

Table2: Experimental conditions

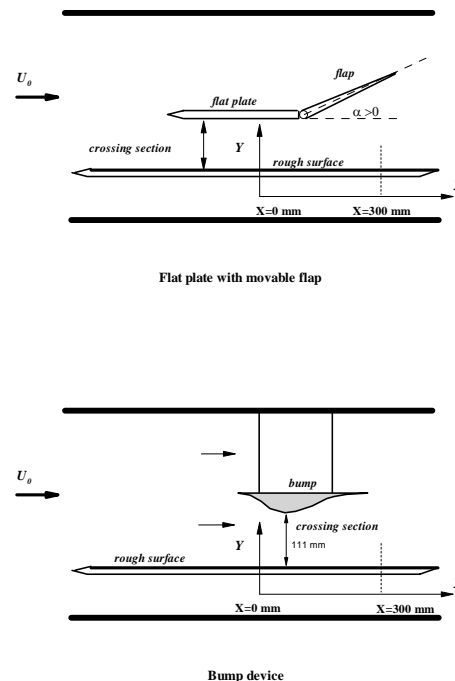


Figure 1: Experimental devices

## ROUGHNESS CHARACTERISTICS

The rough covering surface is composed of sand-paper the chosen roughness of which (*rug1* and *rug2*) is 0.5 mm and 0.6 mm height respectively. A photography of the two rough samples (figure 2) shows the difference in geometry and distribution of the roughness.



Figure 2: Samples of rough surfaces

A valuation of the grain density ( $N/S=240$  grains/cm<sup>2</sup> and 16 grains/cm<sup>2</sup> for *rug1* and *rug2* respectively) allows the spacing parameter  $l/h$  to be calculated. From the values of  $r = (\frac{A_s}{A_p})^{4/3}$  given by Blanchard (1977) relating to

cones, cylinders or tetrahedral we chose for *rug1*, which roughness elements exhibit in a general way elongated form, a mean value  $r=2$ . As for surface *rug2* mainly constituted of pyramidal elements a value of  $r=2.7$  issued from Blanchard (1977) was adopted. The characteristics of the two chosen surfaces are given in table 1.

|      | $l/h$ | $r$ | $\Lambda$ | $h_s/h$ | $h$  | $h_s$ |
|------|-------|-----|-----------|---------|------|-------|
| Rug1 | 1.28  | 2   | 2.56      | 0.57    | 0.50 | 0.29  |
| Rug2 | 4.17  | 2.7 | 10.2      | 1.68    | 0.60 | 1.00  |

Table 1: Test surfaces characteristics

## Cf AND $\Delta u^+$ DETERMINATION

The analysis of roughness effects on the boundary layer characteristics required careful measurements. Different procedures in the determination of wall shear stress from rough-wall mean velocity profiles were tested. On smooth surface, the friction coefficient can be derived from the classic logarithmic law:

$$\frac{U}{U_e} = \frac{\gamma}{\kappa} \ln(y) + \frac{\gamma}{\kappa} \ln\left(\frac{\gamma U_e}{\nu}\right) + \gamma C$$

with  $\kappa = 0.41$  and  $C = 5.25$ . On a rough surface, two additional unknown quantities  $\Delta u^+$  and  $e$  interfere in the logarithmic law which takes the form:

$$\frac{U}{U_e} = \frac{\gamma}{\kappa} \ln(y+e) + \frac{\gamma}{\kappa} \ln\left(\frac{\gamma U_e}{\nu}\right) + \gamma C - \gamma \Delta u^+$$

$e$  corresponds to a shift of the wall due to the presence of the roughness and  $\Delta u^+$  to a shift of the logarithmic region with respect to the smooth case. The common method to determine  $e$ ,  $\gamma$  and  $\Delta u^+$  is based on the preliminary determination of  $e$  (independently of  $\gamma$  and  $\Delta u^+$ ) from the

linear form of the graph ( $U/U_e, \ln(y+e)$ ) in the logarithmic region of the velocity profile as recommended by Perry and Joubert (1968). Then, the slope of the straight line nearer the logarithmic region gives  $\gamma$  whereas its intercept provides  $\Delta u^+$ . When the mean quadratic deviation between the experimental velocity profile and the associated line issued from a least square analysis, estimated on the rough surface, is comparable to the one calculated on the smooth surface, the shift value  $e$  can be neglected (Trijoulet, 1999). In the present experiment the wall shift  $e$  was estimated; its effect seemed to be much weaker than that of the roughness function  $\Delta u^+$  and was thus neglected.

## RESULTS AND DISCUSSION

### Zero pressure gradient boundary layer

The first experiments were conducted on smooth surface in order to be used as reference ones in the analysis of the roughness effects. A comparison of the velocity profiles relating to smooth and rough (*rug1*) surfaces in C1 test case are given in figure 3.

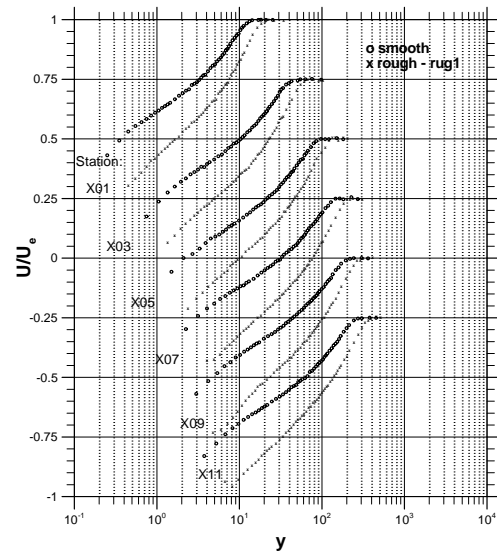


Figure 3: ZPG - Velocity profiles on smooth and *rug1* surface

The velocity profiles for each measurement station are shifted along abscissa and ordinate axis ( $\log 20$  and  $0.25$  respectively) to preserve the plot visibility. The roughness effect is clearly denoted with an important decrease of the velocity throughout the boundary layer.

Figure 4 gives a comparison of the turbulence intensity  $\sqrt{u'^2}/U_e$ . The wall roughness increases the turbulence level throughout the boundary layer. Moreover, the rough surface strongly modifies the ZPG turbulent profiles close to the wall.

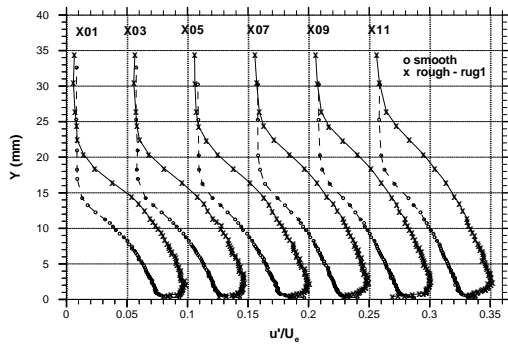


Figure 4: ZPG – Turbulence profiles

Measurements on *rug1* surface were also undertaken in C2 test case conditions corresponding to a Reynolds number  $Re=1.10^6$ . The Reynolds number decrease leads to a weakening of the roughness effect in the boundary layer. A comparison of the velocity profiles at fixed  $y/\delta$  height indicates that  $U/U_e$  increases when the Reynolds number decreases. The roughness effect being less important, the velocity profile come near the smooth reference one.

The evolutions of the skin friction coefficient measured on the *rug1* surface in C1 and C2 configurations are given in figure 5.

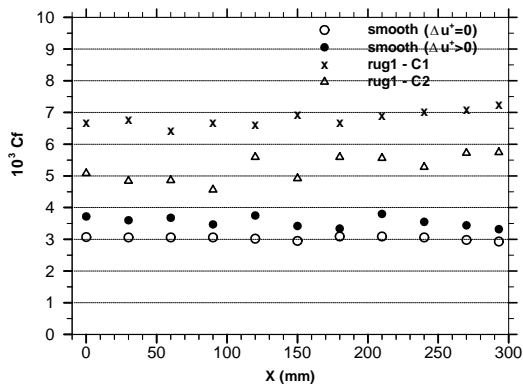


Figure 5: ZPG – Skin friction coefficient evolution

The results relating to the smooth reference case, for which the agreement with the Ludwig-Tillmann law evolution was verified, are also indicated. The measurement results on *rug1* surface confirm the previous purpose concerning the Reynolds number effect; in C2 configuration, the mean value of the skin friction coefficient is close to  $5.5 \cdot 10^{-3}$  while it reaches  $7.0 \cdot 10^{-3}$  in C1 test case.

The algorithm dedicated to skin friction calculation on rough surfaces from logarithmic law analysis was applied to the smooth case. This algorithm where  $\Delta u^+$  is not forced to be equal to zero applied to the measurement on a smooth surface is more sensitive than the classical data reduction method generally used in smooth cases. This is equivalent to use the classical logarithmic law with a  $C$  constant different of its usual value. The deviations observed on the skin friction evolutions (in the smooth reference case) according as the velocity defect function is zero or not

(figure 5), point out the difficulty in skin friction evaluation from the logarithmic law analysis.

The velocity defect function  $\Delta u^+$  (figure 6), closely constant with  $X$ , increases from 6 to 10 when the Reynolds number increases from  $1 \cdot 10^6$  to  $2 \cdot 10^6$ .

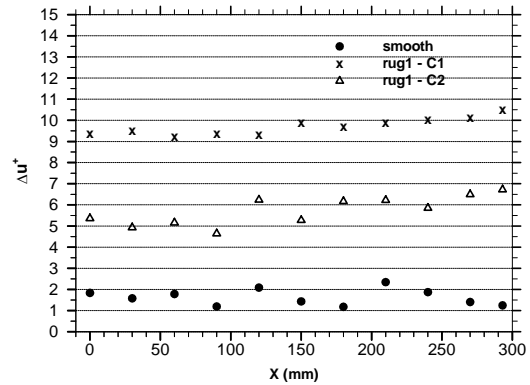


Figure 6: ZPG – Velocity defect function

The Nikuradse correlation gives the variations of the velocity defect function from the roughness Reynolds number :

$$\Delta u^+ = \Delta u^+(h_s^+)$$

$\Delta u^+$  variations being monotonous, this correlation can be inverted. If  $u_\tau$ ,  $\kappa$  and  $C$  are given,  $\Delta u^+$  is obtained from the mean velocity profile using the Clauser logarithmic law. Then, the equivalent sand grain height  $h_s$  can be estimated from the inverted Nikuradse relation.

The equivalent sand grain roughness parameter  $h_s^+$  is close to 150 at the first measurement stations and grows up to 200 at the last measurement station in C1 experimental condition; in C2 configuration,  $h_s^+$  varies from 25 to 50. The decrease of  $h_s^+$ , correlated with the decrease of the Reynolds number, indicates the change of flow regime from fully to transitionally rough.

The evolution of  $h_s/h$  (related to *rug1*) for the two C1 and C2 experimental conditions is given in figure 7.

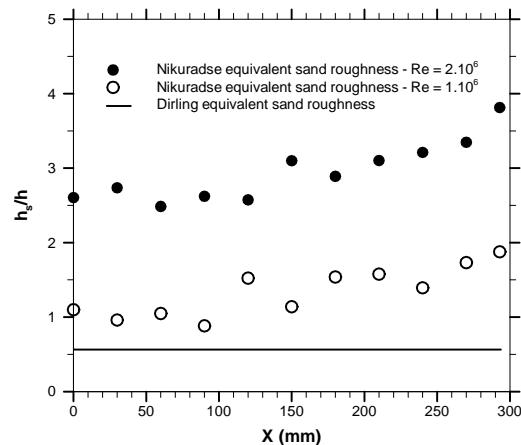


Figure 7: ZPG – Evolution of  $h_s/h$  (*rug1* surface)

As an unexpected result,  $h_s/h$  is strongly dependent upon the Reynolds number; its value is far from the one given by Dirling (1973) and only based on the geometric characteristics of the roughness. This result evidences, for a given roughness, the variation of the equivalent-sand-grain height according as the roughness effect is strong ( $h_s^+ \approx 150$ ) or weaker ( $h_s^+ \approx 30$ ).

The last experiments in ZPG boundary layer were performed on the *rug2* rough surface. This surface differentiates from the previous rough *rug1* by a higher roughness ( $h=0.60$  mm) and a larger grain spacing. In spite of this new rough topology, the boundary layer velocity profiles are little different from the measured ones on *rug1* surface. The rough regime characteristics for the two reference surfaces were compared. The equivalent sand grain roughness parameters  $h_s^+$  are very close but the evolution of  $h_s^+$  seems to be more noisy on *rug2* surface. The evolution of  $h_s/h$  is somewhat chaotic but a mean value close to 2 can be retained not too far from 1.6 obtained from Dirling correlation.

### Adverse pressure gradient boundary layer

The local non-dimensional acceleration parameter  $K$ , given by:

$$K = \frac{v}{U_e^2} \frac{dU_e}{dx}$$

indicates that the slowing-down of the flow is stronger with the bump in the first part of the investigated region, i.e. up to  $X=0.10$  m, than it is with the flap. Beyond this measurement station, the two experimental devices give a quite equivalent pressure gradient. The lowest  $K$  value close to  $-0.5 \cdot 10^{-6}$  considered in this investigation indicates that a strongly decelerated flow is created.

Boundary layer probings on the reference smooth surface were performed with the two pressure gradient arrangements. The velocity profiles in logarithmic form  $u^+ = f(y^+)$  are given in figure 8 for the bump device.

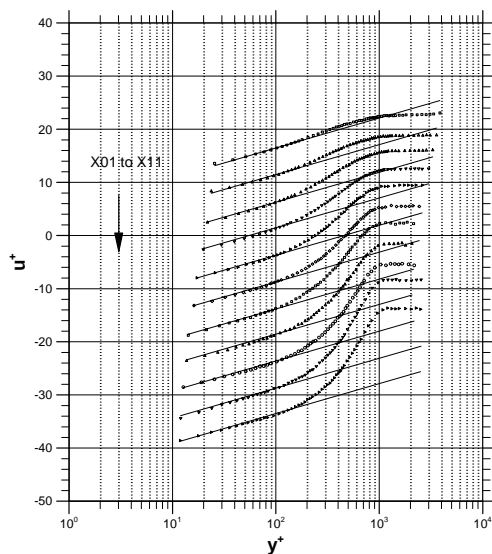


Figure 8: APG – Velocity profiles on smooth surface

At the first measurement stations, the experimental points in the outer part of the boundary layer are very near and even underneath the logarithmic straight line indicating the acceleration of the flow. Quickly, the boundary layer responds to the slowing-down of the external flow: the velocity profiles exhibits a Coles “wake law” evolution typical of decelerated flows. Moreover, the extend of the logarithmic region is less important than it was in ZPG configuration.

The presence of the rough surface seems to modify the pressure gradient effect on the behaviour of the boundary layer mean velocity profiles (figure 9).

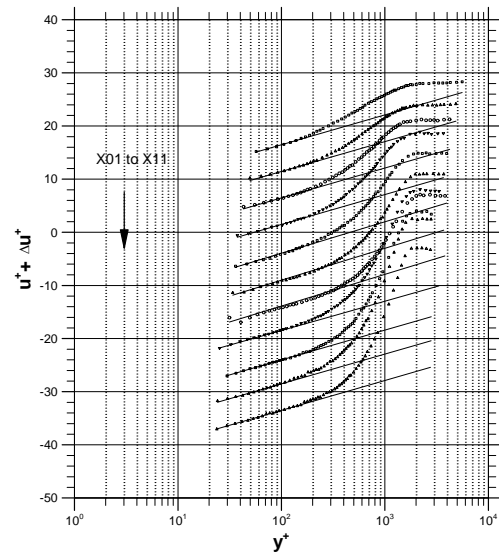


Figure 9: APG – Velocity profiles on rug1 surface-

In a general way, the logarithmic region remains perfectly defined whereas the “wake region” becomes more pronounced than it was in smooth configuration.

The friction coefficient evolutions obtained on the rough (*rug1*) and reference smooth surfaces were compared for the two decelerated flows generated by FD and BD devices set in the test section (figure 10).

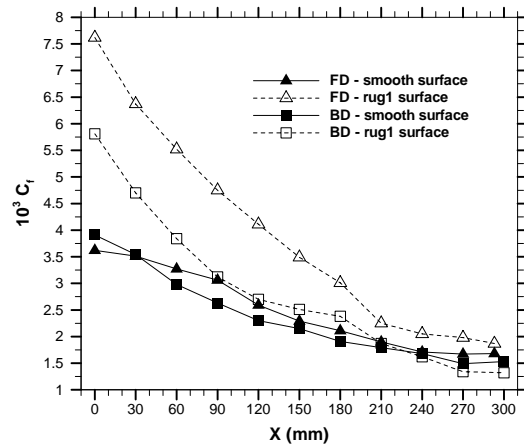


Figure 10: APG – Friction coefficient evolution

In smooth case, the two decelerated flows provide a quite similar decrease of the skin friction. The presence of the rough surface modifies the friction level at the wall and seems to modify the pressure gradient intensity and its effect on the boundary layer flow.

The equivalent sand-grain parameters  $h_s^+$  relating to the two APG flows are quite identical up to  $X=0.12m$ ; beyond this  $X$  location, the noticeable deviations occurring between  $h_s^+$  values point out the difference between the two decelerated flows. Consequently, the ratio  $h_s/h$  grows from 1.5 to 4 in BD flow case (figure 11) whereas a mean value close to  $h_s/h=3$  can be adopted in zero pressure gradient flow. This variation of  $h_s/h$  depending both of the considered  $X$  location and the nature of the pressure gradient is an unexpected and interesting result.

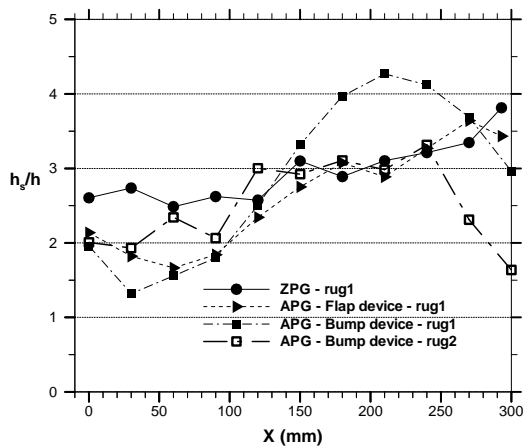


Figure 11: APG – Evolution of  $h_s/h$

In the last part of this experimental study, measurements in APG flow generated by the bump device were undertaken on the *rug2* surface. The measurement results are summed-up by the evolution of  $h_s/h$ , the characteristic parameter of the roughness wall. This evolution is compared to the previous one related to the *rug1* surface in figure 11. The  $h_s/h$  values are different in the second part of the investigated region: a mean value of  $h_s/h=2.2$  and  $3.6$  could be retained for the *rug2* and *rug1* surface respectively. From these results, it would seem that when the flow is submitted to a strong adverse gradient, the boundary layer is sensitive to the combined effects of roughness and pressure gradient.

## CONCLUSION

An experimental study of the boundary layer developing on a rough surface and submitted to an adverse pressure gradient was undertaken. Two different random roughness surfaces were tested. The first lesson we can draw from the results documented in this study was the strong dependency of the rough flow to the Reynolds number in zero pressure gradient. The roughness function increases roughly from 6 to 9.5 when the Reynolds number varies from  $1 \cdot 10^6$  to  $2 \cdot 10^6$ . Correlatively, the roughness Reynolds number  $h_s^+$  based on the Nikuradse equivalent sand grain roughness grows from 40 up to 160. So, the characteristic ratio  $h_s/h$  varying from 1.5 to 3 is far from the 0.6 constant value

depending only of the roughness geometry as predicted by the Dirling correlation.

Useful information were obtained about the combined effects of the pressure gradient and the wall roughness on the development of the boundary layer. The equivalent sand grain roughness Reynolds number seems to be dependent upon the external flow conditions; the  $h_s/h$  ratio growth under strong adverse pressure gradient is significant. Another feature of the adverse pressure gradient is that its impact on the rough flow depends on the nature of the wall roughness.

Nevertheless, these experimental statements must be cautiously interpreted. The accuracy of the ratio  $h_s/h$  depends on the potential uncertainty in the valuation of the velocity defect function and consequently of the skin friction coefficient. We estimated that  $\pm 0.05$  mm uncertainty on the separating distance between the roughness top and the nearer probe location from the wall, could occasion up to  $\pm 12\%$  uncertainty on the skin friction coefficient and the velocity defect function  $\Delta u^+$ . As a result, an uncertainty in the range of  $\pm 20\%$  on the equivalent sand grain roughness height estimating should be possible. These uncertainties do not probably question the results of the present experimental study but they show that no criterion about the variation of the equivalent sand grain roughness can be expected. The main instruction emanating from this experimental investigation is that the use of the equivalent sand roughness concept in rough flow analysis requires that as well the roughness topology (element shape and spacing) as the nature of the flow would be accounted for.

## REFERENCES

- Aupoix, B., Spalart, P. R., “Extensions of the Spalart-Allmaras Turbulence Model to Account for Wall Roughness”, *International Journal of Heat and Fluid Flows*, Vol. 24, pp. 454-462, 2003.
- Blanchard, A., “Analyse expérimentale et théorique de la structure de la turbulence d’une couche limite sur paroi rugueuse”, Thesis, Poitiers University, 1977.
- Dirling, R. B., “A method for computing roughwall heat transfer rates on reentry nosetips”, *AIAA 8<sup>th</sup> Thermophysics Conference*, pp. 73-763, Palm Springs, California, July 1973.
- Nikuradse, J. “Law of flow in rough pipes”, Technical Memorandum 1292, National Advisory Committee for Aeronautics, Washington, 1933.
- Perry, A. E., Joubert, P. N., “Rough-wall boundary layers in adverse pressure gradients”, *Journal of Fluid Mechanics*, Vol. 17, pp. 193-413, 1968.
- Trijoulet, A., “Étude expérimentale de couche limite sur paroi rugueuse”, Thesis, ENSAE Toulouse, 1999.